# New Quadratic Self-Assembly of Double-Decker Phthalocyanine on Gold (111) Surface : from Macroscopic to Microscopic Scale

M Farronato, I. Bidermane, Johann Lüder, Marcel M Bouvet, Adriana Vlad, A Jones, J Simbrunner, R. Resel, B. Brena, Geoffrroy Prévot, et al.

# New Quadratic Self-Assembly of Double-Decker Phthalocyanine on Gold (111) Surface : from Macroscopic to Microscopic Scale

M. Farronato,[†] I. Bidermane ,[a,‡] Johann Lüder,[b,¶] M. Bouvet,[§] A. Vlad,[‖] A. Jones,[⊥] J. Simbrunner,[⊥] R. Resel,[⊥] B. Brena,[‡] G. Prévot,[†] and N. Witkowski[*,†]

†*Sorbonne Université, UMR CNRS 7588, Institut des Nanosciences de Paris, 4 Pl. Jussieu, F-75005 Paris, France*

‡*Department of Physics and Astronomy, Uppsala University, BOX 516, SE-75120 Uppsala, Sweden*

¶*Department of Physics and Astronomy, Uppsala University, Box-516, 75120 Sweden*

§*Institut de Chimie Moléculaire de l'Université de Bourgogne (ICMUB),CNRS UMR 6302, Université de Bourgogne, F-21078 Dijon, France*

‖*Synchrotron SOLEIL, L'Orme des Merisiers, Saint-Aubin, 91192 Gif sur Yvette, France*

⊥*Institute of Solid State Physics, Graz University of Technology, A-8010 Graz, Austria*

E-mail: nadine.witkowski@sorbonne-universite.fr

[a]Current address : Institute Methods and Instrumentation for Synchrotron Radiation Research, Helmholtz-Zentrum Berlin - Bessy II, Albert-Einstein-Strasse 15, D-12489 Berlin, Germany

[b]Current address: Department of Mechanical Engineering, National University of Singapore, Block EA #07-08, 9 Engineering Drive 1, Singapore 117576

**Abstract**

Unveiling the self-organization mechanism of semiconducting organic molecules onto metallic surfaces is the first step to design hybrid devices in which the self-assembling is exploited to tailor magnetic properties. In this study, double-decker rare-earth phthalocyanines, namely lutetium phthalocyanine ($LuPc_2$), are deposited on Au(111) gold surface forming large scale self-assemblies. Global and local experimental techniques, namely grazing incidence X-ray diffraction and scanning tunneling microscopy, supplemented by density functional theory calculations with van der Waals corrections, give insight of the molecular structural arrangement in the thin film and the self-organization at the surface. Our results show unambiguously that the two plateaus of the double-decker phthalocyanine present a different rotation than the isolated molecule. This is evidenced by density functional theory simulations of optimized $LuPc_2$ monolayer showing a perfect agreement with experimental findings. Moreover, the stabilized structure of double layers reveals an eclipsed configuration of the molecules in the stacking, having the ligand plateaus parallel to the gold surface. The high crystallinity of the molecular assembly and its weak electronic coupling with the metallic substrate is expected to open new perspective in the design of opto-electronic or magnetic devices.

# Introduction

Phthalocyanine molecules have been the subject of a large number of investigations due to their versatile applications in the areas such as photovoltaic materials, light-emitting diodes, solar and fuel cells.[3–6] More recently, magnetic phthalocyanines and related molecules, have attracted much attentions for organic spin valve devices,[7] Kondo coupling,[8] spin-state manipulation[9] and even molecular quantum bits.[10] Because magnetic correlations are strongly affected by molecular arrangement and interaction at interfaces, there is an evident need to characterize the molecular architecture of active organic molecules on standard metallic

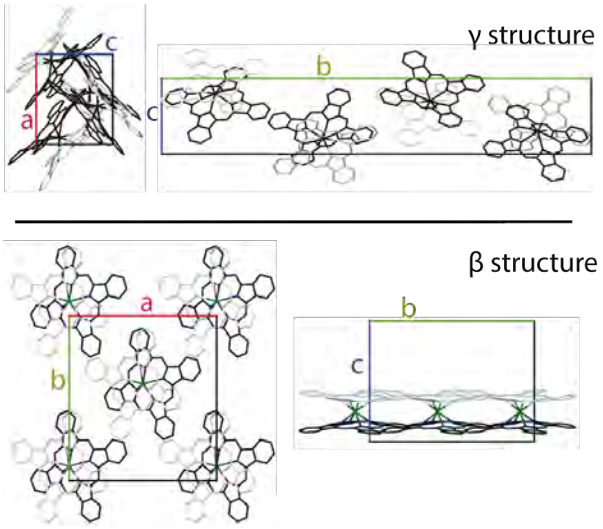


Figure 1: Top : $\gamma$ structure space group $P2_12_12_1$ from $LuPc_2$ $a = 10.553$ Å, $b = 50.795$ Å, $c = 8.959$ Å, taken from Ref.[1] ; bottom: $\beta$ structure space groupe C2/c from $NdPc_2$ $a = 19.01$ Å, $b = 19.066$ Å, $c = 15.538$ Å, $\beta = 116.10°$ taken from Ref.[2] The higher plateau of double-decker phthalocyanine is represented with lighter colors for clarity.

surfaces such as gold. This would result in a detailed knowledge and understanding of the molecule-molecule interactions as well as molecule-surface interactions and possible charge transfer.

A large number of investigations have already been carried out on metal phthalocyanines (MPcs) on gold substrate with the aim to characterize the interface between the gold and the MPcs.[11–14] In these studies, MPcs are found to form closed-packed self-organized two dimensionally (2D) ordered areas at monolayer coverage with flat-lying molecules. In successive adlayers the molecules either adsorb flat or tilted, depending on the central metal cation of the phthalocyanine. Unfortunately, these single decker molecules are sensitive to oxydation that can occur on the central ion, degrading their electrical and magnetic properties. This limitation can be detered by the use of double-decker phthalocyanines, as shown in a recent article.[15] In the study presented here, we focus our interest on a lanthanide double-decker phthalocyanine of lutetium ($LuPc_2$). Each molecule is composed of two identical phthalocyanines, rotated by 45° against each other, and bridged via a Lu(III) ion. Because of that particular geometry, only peripheric ligands are mainly affected upon adsorption on reactive

surfaces,[16] preserving the intrinsic electronic properties of the molecule.

The crystalline structures of double-decker phthalocyanines, are presented in Fig.1. The most stable structure for $LuPc_2$ in single crystal or powder corresponds to the $\gamma$ structure[1] whereas the $\beta$ structure is observed for other rare earth double-decker phthalocyanines.[2] Despite recent studies focusing on double-decker phthalocyanines on metal or semi-metal surfaces,[17–21] none of them are dealing with $LuPc_2$ on Au(111) surface, addressing the global and local structural arrangement of multilayers in relation with the substrate and the microscopic electronic structure of the HOMO and LUMO states in closed-packed multilayers. In this work, the combination of grazing incidence X-ray diffraction (GIXD), scanning tunneling microscopy (STM) and density functional theory (DFT) calculations, allows us to give a comprehensive understanding of $LuPc_2$/Au(111) system. The structure and the orientation of the closed packed molecular architecture with respect to the substrate crystallographic directions is revealed by using GIXD, showing a square in-plane lattice. The self-assembly is unveiled at molecular scale by STM, revealing a rotation of the two ligand plateaus for minimizing self-assembly energy. In the multilayer stack, an eclipsed configuration is evidenced thanks to unique DFT calculations carried out on a self-assembled double layer of $LuPc_2$.

# Experimental and Theoretical Methods

## Sample preparation

The Au(111) single crystal used for the experiments was provided by Surface Preparation Laboratory company. The gold surface was prepared by repeated sputtering and annealing (at about 650°C) cycles until a sharp pattern was observed by low energy electron diffraction. Under these conditions, the well known Au(111) $22 \times \sqrt{3}$ reconstruction was observed by STM and by GIXD.[22]

$LuPc_2$ was synthesized according to literature methods.[23] All the depositions were performed *in situ* under ultra-high vacuum (UHV) conditions to prevent from sample contamination.

$LuPc_2$ molecules, placed in a Ta pocket resistively heated or in a dedicated evaporator for molecules, were outgassed for a few hours at 250°C until the base pressure of the experimental chambers (low $10^{-10}$ mbar) was recovered. During the molecular deposition, the Ta pocket or the crucible of the evaporator was resistively heated to around 300°C, while keeping the vapor pressure in the low $10^{-9}$ mbar range. Most of the results presented here have been obtained on multilayer deposition followed by an annealing at 300°C for 15 minutes.

## Experimental techniques

STM measurements were performed at room temperature using a set-up consisting of two interconnected chambers for sample preparation and STM measurements, operating at a base pressure of low $10^{-11}$ mbar. A commercial variable temperature STM from Omicron Nanotechnology was used to obtain images in a constant current mode. A tungsten tip used in all the measurements, was first etched *ex situ* in a NaOH solution and afterwards flashed up to about 800°C *in situ* in order to remove the oxide layer. All STM images have been processed using the Gwyddion software.[24]

GIXD experiments have been carried out on the SIXS beamline at the synchrotron SOLEIL,[25,26] the photon energy was set at 11 keV, corresponding to a wavelength $\lambda$ of 1.12714 Å. The molecules were deposed *in situ* in the diffractometer chamber. The optical signature of $LuPc_2$ molecules was checked in real time during the deposition by surface sensitive optical reflectivity.[27] The incident beam has been kept at an angle of 0.4° in order to prevent scattering from the bulk by reducing the penetration depth of incoming X rays. All GIXD measurements have been performed at room temperature, using a point detector. The $h$, $k$, $l$ indices correspond to the surface unit cell of Au(111) with $a = b = \frac{a_0}{\sqrt{2}}$, $c = a_0\sqrt{3}$, $\alpha = \beta = 90°$, $\gamma = 120°$ and $a_0 = 4.078$ Å.

## Theoretical methods

All Density Functional Theory (DFT) calculations are performed with the VASP package, the Perdew-Burke-Ernzerhof (PBE) exchange-correlation functional and the projector augmented wave method.[28–32] The energy cutoff is 450 eV and the van der Waals (vdW) interactions are computed with the Tkatchenko-Scheffler method.[33] Structure optimizations are performed until all forces are less than 0.01 eV / Å. The optimizations are carried out to relax structures and volumes for the mono (double) layer of $LuPc_2$ molecules. Free standing mono (double) layers are considered in this study to model the self-organization of the molecules driven by vdW forces in multilayer regime.[16,34,35] For single molecule calculations, only the $\Gamma$ point of the Brillouin zone is computed and the structure of the molecule is optimized while the volume and shape of the simulation cell with a size of $28 \times 28 \times 28$ Å , are kept constant. For mono (double) layers, the simulation cell contains 1 (2) molecule(s) and the vertical distance, labeled as $z$, between molecules of neighboring simulation cells is kept to at least 12 Å. The initial lateral dimensions of the mono (double) layer is assumed to be 17 Å in both directions forming a quasi-square lattice on the $LuPc_2$ monolayer. The assumption of a quasi-square lattice is motivated by recent studies of metal-free Pc molecules adsorbed on Au(111) forming a similar quasi-square lattice[36] and by the present study using GIXD. The Brillouin zone is sampled with Monkhorst-Pack scheme of $3\times$ $3\times$ 1 $k$-points where the periodic direction of the mono (double) layer is assumed in $x$ and $y$. Double layers of $LuPc_2$ molecules are studied with two free standing monolayers, one adsorbed on the other (adsorption direction is $z$). Because the adsorption potential of two $LuPc_2$ monolayers is expected to be dominated by vdW interactions[16] and the adsorption surface area is relatively large (e.g. 13.4 Å$\times$13.4 Å for the optimized free standing monolayer as discussed below), several local minima in the potential separated by shallow potential barriers can occur. Thus, we sample several adsorption structures by shifting the upper $LuPc_2$ monolayer over a grid of points with a resolution of 0.75 Å in $x$- and $y$-direction. Only a quarter of the unit cell is sampled due to the symmetry of the structure. We assume that no rotation of molecules in

the upper and lower layer occurs with respect to each other. The initial separation distance between the two layers is 3.5 Å.

With the total energies of the optimized single molecule ($E^s$) and of the mono (double) layer ($E^{m(d)}$), the formation energy per $LuPc_2$ molecule can be estimated as

$$E_f^{m(d)} = (E^{m(d)} - nE^s)/n$$

where $n$ is the number of molecules in the layer. The adsorption energy ($E_{ad}$) of one monolayer attached onto the other can be expressed as

$$E_{ad} = (E_f^d - nE_f^m)/n.$$

The band decomposed charge density (BDCD) method can be used to simulate STM images. Within this method, the conductivity is assumed to be proportional to the charge density within an energy window determined by the bias voltage. The bias voltage in experimental measurements is associated with the bias energy in the BDCD method. The charge density within a certain energy window, e.g. from HOMO to 2 eV below HOMO, can be obtained by summation of the densities over all $k$-points of the states within this energy range. The summation can be carried out over occupied and unoccupied states relative to a selective energy level, here we choose HOMO or the valence band maximum (VBM). Then, a 2D density profile is taken from BDCD at height of $z$ the simulation cell, which can be used to qualitatively evaluate experimental STM images. We choose to take the density profile at a height of 2.8 Å above the $LuPc_2$ molecule layer in lateral directions at bias energy of -2 and 2 eV (corresponding to -2 and 2 V bias voltage) around VBM.

# Results and discussion

## Self-organization at macroscopic scale

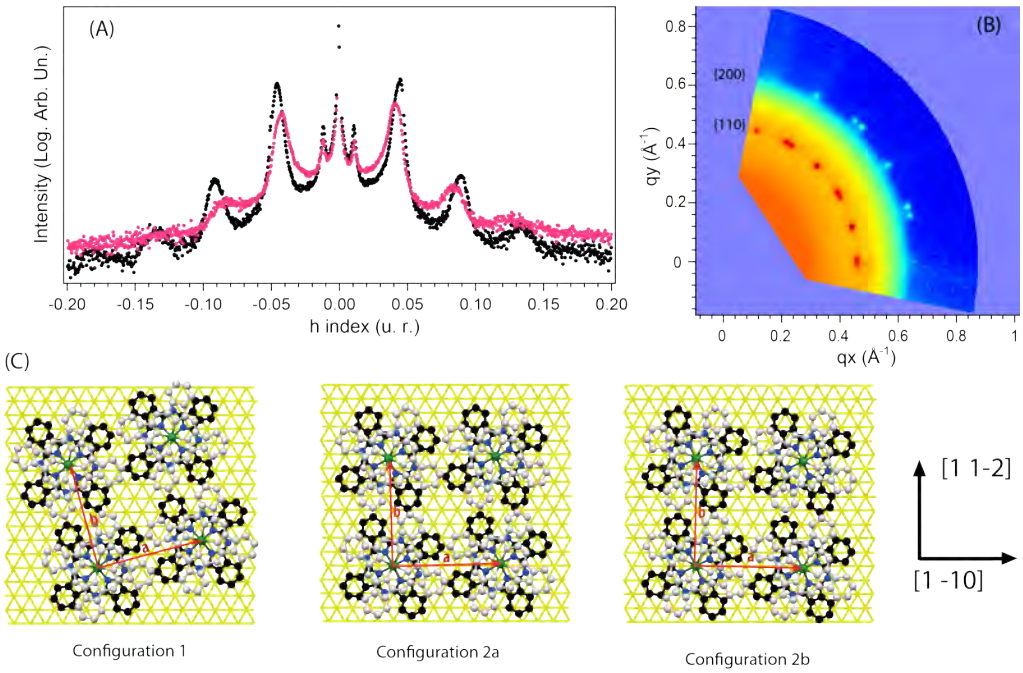


Figure 2: (A) : Scan along the $[1\bar{1}0]$ direction of the reciprocal space of gold before (black dots) and after (pink dots) deposition of molecules. (B) : In-plane mesh ($l$=0.05 Å) of the $LuPc_2$/Au(111) after heating to 285°C. (C) : Representation of inequivalent domains of $LuPc_2$ on Au(111) lattice (colored in yellow), based on the experimentally determined 2D lattice and close packing of the LuPc molecules. The upper plateau $LuPc_2$ has been coloured in light grey for clarity. In-plane molecular distances are represented by plain line red arrows of $a = 13.6 \pm 0.1$ Å, $b = 13.6 \pm 0.1$ Å with an angle of $90 \pm 0.1°$ between the two directions.

The main GIXD results are displayed in Fig.2. The plot in Fig.2(A) shows a scan along the $[1\bar{1}0]$ direction of the reciprocal space, i.e. along the large side of the herringbone reconstruction of gold around the (0,1,0.05) condition. The cut has been plotted versus $h$

index for ease of representation; black dots correspond to the clean gold surface whereas pink dots correspond to the signal measured for a 10 nm thick film of $LuPc_2$, as deposited. The central peak at $h = 0$ corresponds to the intersection of the crystal truncation rod of Au(111); the peaks at $h = \pm 0.012$ reflect the periodicity of the elbow positions appearing on the zig-zag reconstruction along $[1\bar{1}0]$ direction.[22] The peaks found at $h = \pm 0.045$ and $h = \pm 0.09$ are assigned to the first and second order of $22 \times \sqrt{3}$ herringbone reconstruction respectively.[37] Upon $LuPc_2$ deposition, it can be noticed that the peaks related to the gold reconstruction pertains but are smoothed and shifted to lower $h$ values. The attenuation of intensity is attributed to a loss of long range order of the reconstruction, whereas the shift indicates that the period of the reconstruction increases. From the position of the first and second order peaks, we measure an increase of about 4.5 % of the period. A similar result has been obtained by Iski et al. when depositing naphtho[2,3-a]pyrene on Au(111).[38] In their experiments, the period of the herringbone reconstruction was shown to increase from 6.3 nm up to 19 nm. Such variations may be related to a change of surface stress. Indeed, the Au(111) reconstruction corresponds to a densification of the surface plane. It originates from the large value of $(\tau - \gamma)/(a_0 E_c)$ where $\tau$ and $\gamma$ are the surface stress and surface free energy of the non-reconstructed (1×1) surface and $a_0$ and $E_c$ the lattice constant and cohesive energy.[39] When the surface stress decreases, the surface density of the reconstruction is lowered and the period increases. Such surface stress variations are commonly observed upon chemisorption[40] and a reduction of tensile stress is associated with a charge transfer from the substrat to the adsorbate.[39] The surface stress difference between the (1×1) and $(22\times\sqrt{3})$ surfaces has been previously estimated as 0.2 N/m.[41] In the present case, the change of surface stress must be much smaller, of the order of a few mN/m. This is also much smaller than the surface stress variations, of a few N/m, observed when adsorbing a highly electronegative atom on a transition metal surface.[42] This indicates that the charge transfer between Au(111) and $LuPc_2$ is very weak. Such charge transfer has already been evidenced for metal free phthalocyanine on gold by means of X-ray absorption spectroscopy[43] and is

reported here for the first time on double-decker phthalocyanine by using surface diffraction to our knowledge.

The inplane map ($q_\perp$=0.078 Å$^{-1}$, corresponding to $l$=0.07) of one symmetry domain of the molecular layer is displayed in Fig.2(B) on a layer annealed to 285°C, below the sublimation temperature of the molecules. Two series of spots are seen: one at $q_{\|} = 0.461 \pm 0.002$ Å$^{-1}$, corresponding to 110 reflections, and the other at $q_{\|} = 0.653 \pm 0.004$ Å$^{-1}$, corresponding to 200 reflections. The presence of sharp spots clearly indicates a long range order of the molecules in the surface plane that self-organize in a square lattice with a molecule-molecule distance of $13.6 \pm 0.1$ Å. Note that the observed lattice is quite close to the lattice periodicity of the (001) plane of $\beta$-structure of NdPc with $a = b = 13.46$ Å with an enclosing angle of 89.83°.

Looking carefully at the in-plane map, one can note that there is an alternance between single spots and double ones; moreover every double spot of the {110} reflections corresponds a single one in the {200} and reciprocally. The period between two (double or single) spots is rougly 30° whereas the period between two spots (no matter which ones) is about 15°. This accounts for a total of 24 domains, which divided by the 6-fold symmetry of the substrate and considering a 4-fold symmetry of the overlayer, reduces to 2 inequivalent symmetries of orientation. Both inequivalent symmetries are plotted in Fig.2(C), denoted as Configuration 1 and Configuration 2. Both are rotated by an angle of 45° relative to each other. The molecular packing is taken in analogy to the $\beta$-structure of NdPc, in which the two plateaus of the molecule are slightly misoriented with respect to the free molecule. In the Configuration 1, relative to the single peaks of the map, the molecules arrange in a square whose diagonal is aligned with the close packed direction of the gold substrate. In this configuration, the sides of the square (represented as red arrows in Fig.2(C)) are not aligned with high symmetry axes of the gold substrate.

The two configurations labelled (2a) and (2b), corresponding to the twin spots of the map, are generated by a slight misalignement of the molecular square cell of ±1.29° with respect

to the $[1\bar{1}0]$ direction. One side of the square is then almost aligned with the ridges formed by the herringbone reconstruction along $[11\bar{2}]$, while the other is perpendicular to the ridges, along $[1\bar{1}0]$. So far in the literature, all studies report on a configuration similar to configuration (1) in monolayer (ML) or sub-monolayer (sub-ML) self-assemblies of single decker phthalocyanine of FePc/Au(111), $H_2$Pc/Au(111) , CuPc/Au(111), MnPc/Au(111)[13,36,44–46] or in double-decker of $YPc_2$/Au(111).[20] In a STM study of $LuPc_2$/Ag(111), Toader et al. found that the smallest angle between the one unit cell vector of the molecular assembly and one of the equivalent substrate directions was determined to be 15°, corresponding to our finding for the configuration (1).[17] A similar configuration is then expected to occur at the monolayer coverage of $LuPc_2$ on Au(111) as suggested by the GIXD. To our knowledge, no studies report on the observation of the configuration (2) at a ML or sub-ML coverage on gold in which the square lattice formed by the molecule is aligned with the ridges of the herringbone reconstruction of gold. The configuration (1) seems to be driven by the molecule-substrate interaction rather than by molecule-molecule interaction. Very few studies report on the packing of the molecules in the multilayer coverage range from the structural point of view. In a STM study, the authors investigated successive depositions of FePc/Au(111) and evidenced the presence of the packing of both configurations (1) and (2).[13] In the STM images a clear alignement of the molecules along the rigdes of the herringbone reconstruction is observed. Our GIXD measurements indicate clearly the presence of the two configurations in the multilayer, with intensities presenting a ratio of about 2/3 for the two configurations. From the discussion presented above, we can suggest that even if the herringbone influences the nucleation site of the molecular terrasses, it is most likely the hexagonal symmetry of the substrate which acts as a template in the monolayer regime whereas herringbone reconstruction influences the self-organization in the stack. The GIXD measurements allow us to gain the following information regarding $LuPc_2$/Au(111) :

– the herringbone reconstruction pertains upon the adsorption of the molecules but en-

couters a relaxation of about 4.5%, attributed to a small charge transfer from the gold substrate to the molecules.

- the molecules self-organize on the herringbone reconstructed gold surface in perfectly squared in-plane lattice of $13.6 \pm 0.2$ Å which is close to the molecular packing present in the $\beta$ structure.

- two main orientations of the molecular lattices with respect to the substrate are evidenced : either the molecular square lattice is aligned with the dense direction of gold or it is rotated by 15° .

## Self-organization at microscopic scale

In a similar experiment, STM images recorded at room temperature on an annealed multilayer, are displayed in Fig.3. The top image (Fig.3(a)) corresponds to an area of 100 nm$\times$23.6 nm where a large terrace of self-organized molecules is observed. Height profile along the solid line is presented in Fig.3(b) and a zoom of the framed region is shown in Fig.3(c).
On the large terrace seen in the top image (Fig.3(a)), scarce individual molecules, appearing as white protrusions, are resolved. The terrace has sharp but irregular edges and presents extended defects (holes) interpreted as missing molecules in the self-assembly. The most interesting feature is evidenced by the height profile seen in the Fig.3(b). From the left side, a first protusion of about 2.5 Å corresponding to a single molecule sitting on the underneath layer is seen. Then a step of about 6 Å is measured when reaching the terrace, with a step down of about 2.5 Å , when crossing the side of the inner hole in the terrace. Because the step from the lower layer to the upper terrace corresponds to about twice the height of a single molecule, the terrace is interpreted as composed of a double layer of $LuPc_2$ molecules. This trend has been systematically observed on different samples after annealing but also for the as-deposited multilayers. This behavior is intriguing and has not been reported so far for

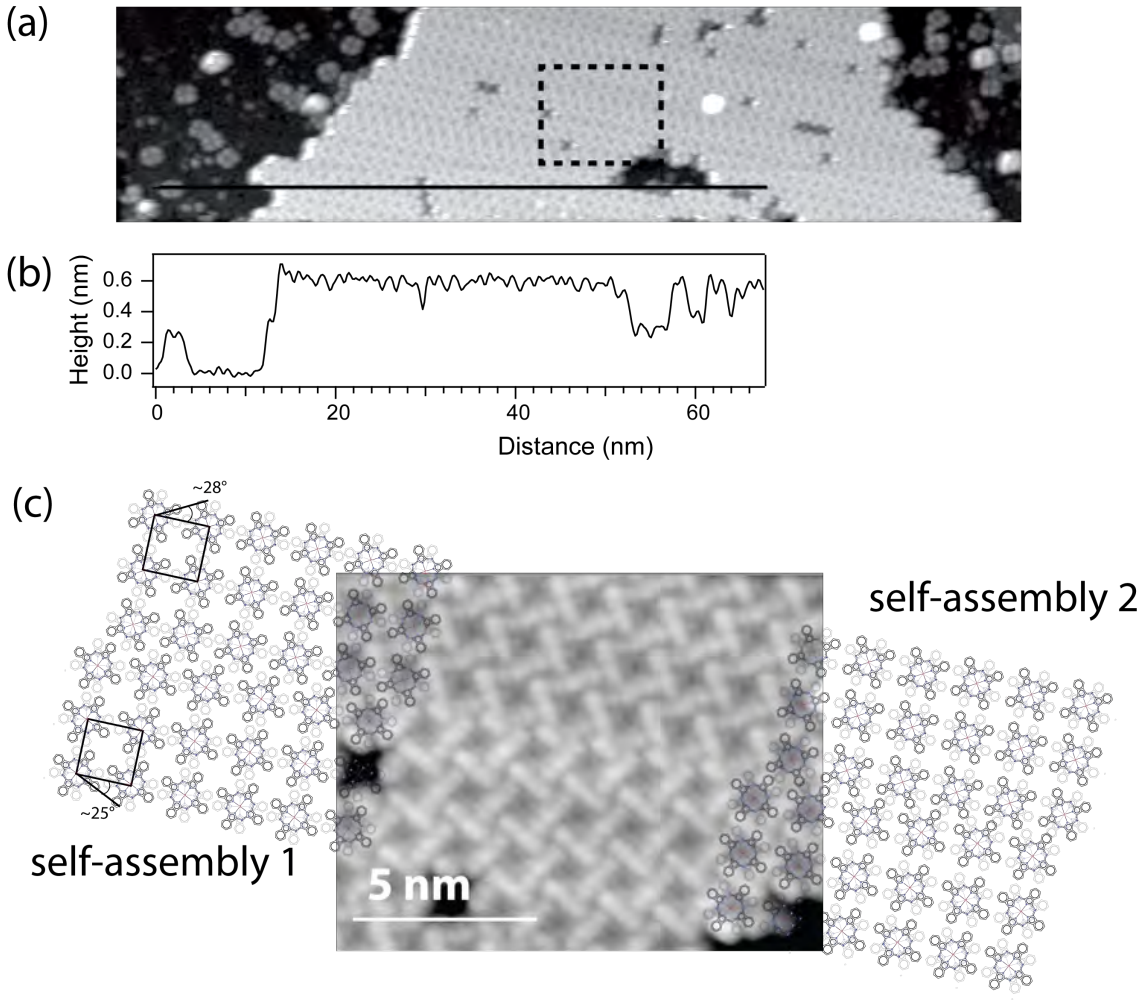


Figure 3: STM image recorded on $LuPc_2$ multilayer after annealing (-2.6 V, 700 pA); (a) large scale image of area 100 nm×23.6 nm: (b) : height profile along the solid line drawn in the large scale image; (c) zoom region framed in the large scale image.

double-decker phthalocyanines to our knowledge. Such bilayer formation has been already reported for the polar molecule of Titanyl Phthalocyanine (TiOPc) deposited Ag(111) for multilayer deposition. In the observed bilayers the two titanyl groups are facing each other in a staggered configuration where the negatively charged oxygen of each group faces the hydrogen of the benzene group, stabilizing the bilayer.[47] In $LuPc_2$/Au(111), the sharpness of the terraces edges points toward a stacking in which the central ions are superimposed in an eclipsed configuration as it will be discussed later.

Looking at the zoomed image in Fig.3(c), the molecules clearly self-organize in two domains that have been separated by a dashed line for the sake of clarity. The two domains present a square lattice of identical parameters and orientation, in agreement with GIXD observations. The axis linking two opposite phenyl groups of the upper plateau (denoted as phenyl symmetry axis) is rotated by about 26° clockwise or counterclockwise with respect to the side of the square lattice, for the upper and lower domain respectively, as sketched in the self-assembly 1. To go further in the understanding of the 2D packing, two self-assemblies can be proposed to interpret the STM observation. Considering a molecular description derived from the $NdPc_2$ resolved by XRD in the $\beta$ configuration,[2] in which the lower plateau of the molecule presents a rotation of about 37° compared to the upper one (instead of the 45° in the isolated form), two arrangements of molecules can be considered to restitute the STM measurement for the two domains. The two self-assemblies, sketched in the Fig.3(c), are proposed. They only differ in the rotation of the lower plateau with respect to the upper one (clockwise for self-assemby 1 and counterclockwise for self-assemby 2), i.e. the molecules are flipped from one model to the other of the same domain. The molecules need to be flipped in the second domain below the dashed line to preserve the orientation of the square lattice. Differences are observed in the two proposed models regarding the respective positions of the lower plateaus : in the self-assemby 1, the lower phenyl groups of adjacent molecules are in close contact which is unlikely to occur due to steric effect and hydogen repulsion whereas in the self-assemby 2, the phenyl groups are distant, making this configuration a more favorable

one. It is worthwile to note that in self-assemby 2, the symmetry axis of lower phenyl from one domain is aligned with the upper one of the other domain, inducing an identical packing for the upper and lower plateau. From this first qualitative analysis, the self-assemby 2 configuration seems to be favorable to reproduce the observed STM arrangement.

In order to validate the above experimental finding on multilayer, simulations of STM images at positive and negative bias using DFT have been performed on a suspended single layer of $LuPc_2$ in vacuum and the results are presented in Fig.4. The stabilized packing obtained

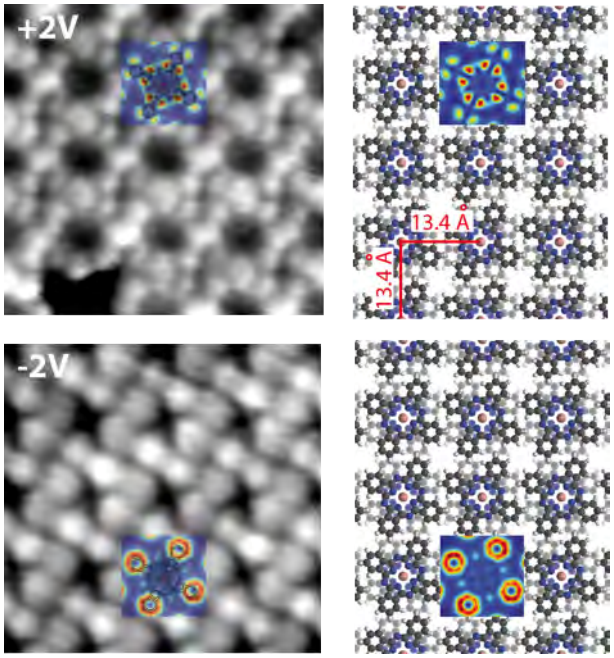


Figure 4: Left: Experimental STM image recorded on multilayer of $LuPc_2$/Au(111) for a sample bias of +2V and -2V; Right : Simulated lattice of monolayer $LuPc_2$ spanning over several cells at biases corresponding to +2 V (top) and -2 V (bottom).

from DFT corresponds to a square lattice of 13.4 Å which is inline with the molecule-molecule distance of 13.6 Å measured by GIXD and which corresponds to the STM finding. The phenyl symmetry axis of the upper plateau appears to be rotated by 26° with respect to square lattice as also observed on the STM measurements (26°- 28° was estimated on experimental STM in Fig.3(c)). Moreover, the lower plateau of the molecule presents a mis-orientation of 37° with respect to the upper one, validating the self-assembly 2 proposed in

the Fig.3(c). The DFT calculations reveal how the self-assembly modifies the distribution of filled and empty electronic states. At a bias of -2 V, the filled states concentrate more on the benzene rings, and only four bright protrusions are observed in both DFT and experimental STM. At a bias of +2V, the empty states are splitted on the side of the pyrolic group, leading to the observation of two distinct lobes of intensity in the calculated and experimental STM image. When compared to the isolated molecule,[48] empty electronic states are now distributed on the four benzene rings equally evidencing a redistribution of the electronic states induced by the self-assembly. The similarities evidenced here can be regarded as a validation of the DFT calculation.

DFT calculations of the self-assembled layer being validated by experimental evidence, we can investigate further the configuration of an adlayer onto the self-assembly, answering the question on how the two molecules in the upper and lower layer are oriented with respect to each other. To that end, DFT calculations have been carried out on double layers of $LuPc_2$ and the results are shown in Fig.5. The optimized structure of the $LuPc_2$ single molecule is shown in Fig. 5(A) (left top). As known from our previous study,[48] the outer parts of phthalocyanine plateaus are bent away from the center of the molecule, leading to a maximal distance between the lower and the upper phthalocyanine plateau of more than 4.3 Å. The optimized structure of the $LuPc_2$ monolayer (Fig. 5(A) right top) shows that. In the monolayer, the phthalocyanine plateaus become flat with a height of less than 3.4 Å that is reduced from 4.3 Å in the free molecule. To our best knowledge, this is the first time that DFT calculations determine accurately the experimental height of $LuPc_2$ molecule. Previously it was assumed that vdW forces could lead to a flattening of the molecular structure or it could be caused by vertical stacking of several double-decker phthalocyanines on top of each other.[48] Here, we additionally show that the lateral interaction to neighboring phthalocyanine in a double-decker formation leads to the flattening of the structure during the monolayer formation, resulting in a lateral extension of the relaxed quasi-square simulation

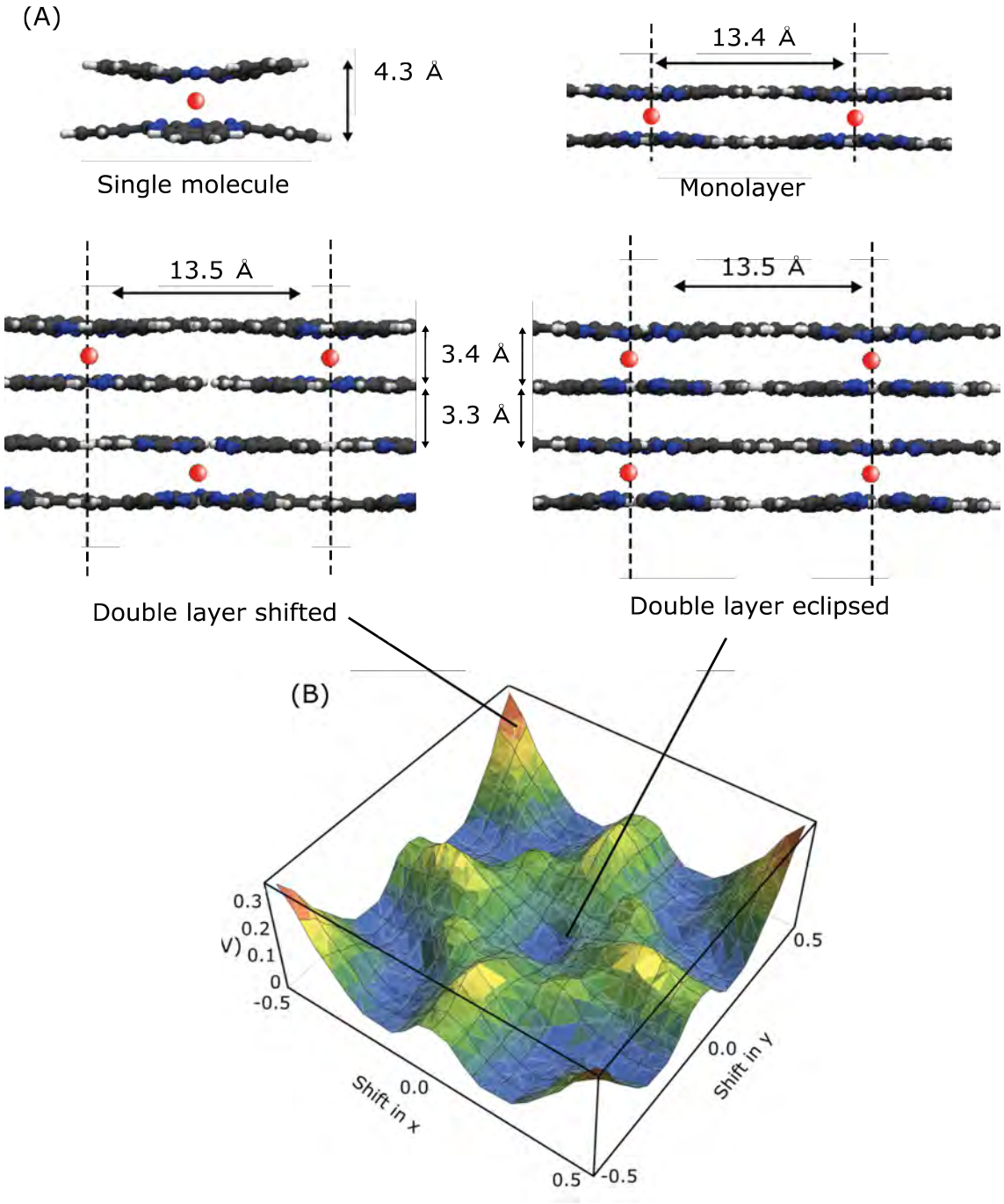


Figure 5: (A) Side view of the optimized structures of the single molecule and the monolayer of $LuPc_2$ as well as the shifted and the eclipsed double layer. The lateral extensions of the simulation cells are indicated with dashed lines. Double arrows show the height of the molecules as well as their separation in the double layers or the simulation cell size. (B) Potential energy surface of shifted double layers in $x$ and $y$ direction measured relative to the global minimum of the computed structures.

cell of 13.4 Å in both directions. In constrast to the single molecule, the two phthalocyanine plateaus are not rotated by 45° to each other, but the contraction of the simulation cell during volume relaxation reduces the angle to 37°, in agreement with the $NdPc_2$ $\beta$ structure.[2] For the double layer, we distinguish between two structures as follows. In the lowest energy structure shown in Fig. 5(A) (middle right), the molecules in the two layers sit on top of each other (eclipsed) resulting in the same orientation of the upper and lower phthalocyanine plateaus in each molecules, respectively; i.e. two adjacent plateaus are rotated by 37°. In the most unstable structure shown in Fig. 5(A) (left middle), the upper $LuPc_2$ layer is shifted by 0.5 lateral lattice vectors in $x$- and in $y$-direction (i.e. [0.5,0.5]) with respect to the lower layer. Both double layer structures have slightly larger lateral lattice vectors of 13.5 Å×13.5 Å getting closer to GIXD finding and a separation between $LuPc_2$ molecules of 3.3 Å which is in-line with the finding of 3.25 Å measured by standard XRD (See Supporting Information).

For the double layer, the computed adsorption potential scan is shown in Fig.5 (B). It has several local minima and one maximal potential height of 300 meV per molecule. For the eclipsed case, that is the minimum of the potential surface, the adsorption energy of one $LuPc_2$ monolayer onto the other is computed to be -1.35 eV per molecule and its formation energy is -2.12 eV per molecule which equals the sum of monolayer formation energy (-0.77 eV) and adsorption energy of two monolayers on each other (-1.35 eV). For the shifted structure, the interaction is weaker: the adsorption energy is -1.07 eV and the formation energy is -1.84 eV.

Both formation energy and changes in electronic structure hint that the mono and the double layer of $LuPc_2$ are governed by vdW forces. These calculations are performed for a particular orientation of the molecules in the two layers with respect to each other, and result in excellent agreement with the experimental finding, providing an insight into the general mechanism in the formation of the interaction between mono and double layer of $LuPc_2$.

Thanks to STM and DFT calculation, local arrangement of the molecules in the layer

and in double layer can be unveiled :

- $LuPc_2$ molecules self-organize in a square lattice forming domains in which molecules are flipped resulting in the same square lattice and arrangement and governed by vdW forces.
- in the self assembly, the two plateaus are rotated by 37 degrees with respect to each other which is an intrinsic result of the monolayer formation.
- double layers are often observed in which the central ions are superimposed in eclipsed configuration with ligand plateau perpendicular to the stacking direction.

# Conclusion

The self-assembling of $LuPc_2$ molecules on Au(111) surface at room temperature is unveiled as a result of combined study using diffraction, scanning tunneling microscopy and density functional theory. GIXD revealed that the herringbone reconstruction of gold pertains upon the adsorption of the molecules, but encouters a relaxation of about 4.5 %, attributed to a small charge transfer from the gold substrate to the molecules. In the multilayer, the molecules self-organize in perfectly squared in-plane lattice of $13.6 \pm 0.2$ Å corresponding to a new quadratic structural phase for double-decker phthalocyanine. STM measurements supported by DFT calculations disclose how the ligand plateaus are mutually arranged within the 2D packing : a rotation of 37° of the two plateaus is unambiguously evidenced. Moreover, unique DFT calculations carried out on self-assembled double-layer confirm that eclipsed configuration is stabilized for 3D packing in which molecules pile up in the upper layer adopting the identical configuration than in the lower one.
Double-decker phthalocyanines appear as ideal candidates to investigate the design of weakly interactive self-assemblies on to close-packed surfaces, including superconducting ones, paving the route to the development of sophisticated logic memories.

## Acknowledgments

We are grateful to SIXS beamline staff for providing support and assistance during the beamtime. We acknowledge the financial support from SOLEIL synchrotron facility, the European Union Seventh Framework Programme under grant agreement n° 607232 THIN-FACE. The authors thank the Austrian Science Foundation (FWF) [P30222] and the Carl Trygger Foundation for financial support and the Swedish Research Council (VR, project grant 2014-3776).

## Supporting Information

Supporting information includes XRD measurements on $LuPc_2$ thick film on Au(111)and extented view of the STM image presented in the figure 3(c).

## References

(1) Moskalev, P. N.; Shapkin, G. N.; Darovskikh, A. N. Synthesis and Properties of Electrochemically Oxidized Dipththalocyanine of Rare-Earth Elements and Americium. *Zh. Neorg. Khim.* **1979**, *24*, 340–346.

(2) Darovskikh, A. N.; Tsytsenko, A. K.; Frankkamenetskaya, O. V.; Fundamensky, V. S.; Moskalev, P. N. Neodymium Diphthalocyanine Polymorphism - the Molecular and Crystal-structure of the $\beta$-phase. *Kristallografiya* **1984**, *29*, 455–461.

(3) Parra, V.; Bouvet, M.; Brunet, J.; Rodríguez-Méndez, M. L.; de Saja, J. A. On the Effect of Ammonia and Wet Atmospheres on the Conducting Properties of Different Lutetium Bisphthalocyanine Thin Films. *Thin Solid Films* **2008**, *516*, 9012.

(4) Bogani, L.; Wernsdorfer, W. Molecular Spintronics using Single-Molecule Magnets. *Nat. Mater.* **2008**, *7*, 179.

(5) Carrette, L.; Friedrich, K. A.; Stimming, U. Fuel Cells: Principles, Types, Fuels, and Applications. *Chem. Phys. Chem.* **2000**, *1*, 162.

(6) Thelakkat, M.; Schmitz, C.; Schmidt, H.-W. Fully Vapor-Deposited Thin-Layer Titanium Dioxide Solar Cells. *Adv. Mater.* **2002**, *14*, 577.

(7) Cucinotta, G.; Poggini, L.; Pedrini, A.; Bertani, F.; Cristiani, N.; Torelli, M.; Graziosi, P.; Cimatti, I.; Cortigiani, B.; Otero, E. et al. Tuning of a Vertical Spin Valve with a Monolayer of Single Molecule Magnets. *Adv. Funct. Mater.* **2017**, *27*, 1703600.

(8) Hiraoka, R.; Minamitani, E.; Arafune, R.; Tsukahara, N.; Watanabe, S.; Kawai, M.; Takagi, N. Single-Molecule Quantum Dot as a Kondo Simulator. *Nat. Commun.* **2017**, *8*, 16012.

(9) Heinrich, B. W.; Ehlert, C.; Hatter, N.; Braun, L.; Lotze, C.; Saalfrank, P.; Franke, K. J. Control of Oxidation and Spin State in a Single-Molecule Junction. *ACS Nano* **2018**, *12*, 3172–3177, PMID: 29489330.

(10) Moreno-Pineda, E.; Godfrin, C.; Balestro, F.; Wernsdorfer, W.; Ruben, M. Molecular Spin Qudits for Quantum Algorithms. *Chem. Soc. Rev.* **2018**, *47*, 501–513.

(11) Barlow, D.; Scudiero, L.; Hipps, K. Scanning Tunneling Microscopy of 1, 2, and 3 Layers of Electroactive Compounds. *Ultramicroscopy* **2003**, *97*, 47.

(12) Takada, M.; Tada, H. Low Temperature Scanning Tunneling Microscopy of Phthalocyanine Multilayers on Au(111) Surfaces. *Chemical Physics Letters* **2004**, *392*, 265.

(13) Cheng, Z. H.; Gao, L.; Deng, Z. T.; Liu, Q.; Jiang, N.; Lin, X.; He, X. B.; Du, S. X.;

Gao, H.-J. Epitaxial Growth of Iron Phthalocyanine at the Initial Stage on Au(111) Surface. *J. Phys. Chem. C* **2007**, *111*, 2656.

(14) Lu, X.; Hipps, K. W. Scanning Tunneling Microscopy of Metal Phthalocyanines: d(6) and d(8) Cases. *J. Phys. Chem. B* **1997**, *101*, 5391.

(15) Farronato, M.; Lder, J.; Longo, D.; Cruguel, H.; Bouvet, M.; Brena, B.; Witkowski, N. High Tolerance of Double-Decker Phthalocyanine Towards Molecular Oxygen. *J. Phys. Chem. C* **2018**,

(16) Bidermane, I.; Luder, J.; Ahmadi, S.; Grazioli, C.; Bouvet, M.; Brena, B.; Martensson, N.; Puglia, C.; Witkowski, N. When the Grafting of Double Decker Phthalocyanines on Si(100)-2 x 1 Partly Affects the Molecular Electronic Structure. *J. Phys. Chem. C* **2016**, *120*, 14270–14276.

(17) Toader, M.; Knupfer, M.; Zahn, D. R. T.; Hietschold, M. Initial Growth of Lutetium(III) Bis-Phthalocyanine on Ag(111) Surface. *J. Am. Chem. Soc.* **2011**, *133*, 5538.

(18) Smykalla, L.; Shukrynau, P.; Hietschold, M. Investigation of Ultrathin Layers of Bis(phthalocyaninato)lutetium(III) on Graphite. *J. Phys. Chem. C* **2012**, *116*, 8008.

(19) Katoh, K.; Yoshida, Y.; Yamashita, M.; Miyasaka, H.; Breedlove, B. K.; Kajiwara, T.; Takaishi, S.; Ishikawa, N.; Isshiki, H.; Zhang, Y. F. et al. Direct Observation of Lanthanide(III)-Phthalocyanine Molecules on Au(111) by using Scanning Tunneling Microscopy and Scanning Tunneling Spectroscopy and Thin-Film Field-effect Transistor Properties of Tb(III)- and Dy(III)-Phthalocyanine Molecules. *J. Am. Chem. Soc.* **2009**, *131*, 9967.

(20) Zhang, Y. F.; Isshiki, H.; Katoh, K.; Yoshida, Y.; Yamashita, M.; Miyasaka, H.; Breedlove, B. K.; Kajiwara, T.; Takaishi, S.; Komeda, T. Low-Temperature Scanning Tunneling Microscopy Investigation of Bis(phthalocyaninato)Yttrium Growth on

Au(111): from Individual Molecules to Two-Dimensional Domains. *J. Phys. Chem. C* **2009**, *113*, 9826.

(21) Vitali, L.; Fabris, S.; Conte, A. M.; Brink, S.; Ruben, M.; Baroni, S.; Kern, K. Electronic Structure of Surface-Supported Bis(phthalocyaninato) Terbium(III) Single Molecular Magnets. *Nano Lett.* **2008**, *8*, 3364.

(22) Barth, J. V.; Brune, H.; Ertl, G.; Behm, R. J. Scanning Tunneling Microscopy Observations on the Reconstructed Au(111) Surface: Atomic Structure, Long-range Superstructure, Rotational Domains, and Surface Defects. *Phys. Rev. B* **1990**, *42*, 9307–9318.

(23) Bouvet, M.; Simon, J. Electrical-properties of Rare-Earth Bisphthalocyanine and Bisnaphthalocyanine Complexes. *Chem. Phys. Lett.* **1990**, *172*, 299.

(24) Necas, D.; Klapetek, P. Gwyddion: an Open-Source Software for SPM Data Analysis. *Cent. Eur. J. Phys.* **2012**, *10*, 181–188.

(25) Baudelet, F.,; Belkhou, R.,; Briois, V.,; Coati, A.,; Dumas, P.,; Et, Al., Soleil a New Powerful Tool for Materials Science. *Oil Gas Sci. Technol.* **2005**, *60*, 849–874.

(26) Coati, A.; Chavas, L. M. G.; Fontaine, P.; Foos, N.; Guimaraes, B.; Gourhant, P.; Legrand, P.; Itie, J. P.; Fertey, P.; Shepard, W. et al. Status of the Crystallography Beamlines at Synchrotron SOLEIL. *Eur. Phys. J. Plus* **2017**, *132*, 174.

(27) Boudet, S.; Bidermane, I.; Lacaze, E.; Gallas, B.; Bouvet, M.; Brunet, J.; Pauly, A.; Borensztein, Y.; Witkowski, N. Growth Mode and Self-Organization of $LuPc_2$ on Si(001)-2$\times$1 Vicinal Surfaces: An optical Investigation. *Phys. Rev. B* **2012**, *86*, 115413.

(28) Kresse, G.; Hafner, J. Ab initio Molecular Dynamics for Liquid Metals. *Phys. Rev. B* **1993**, *47*, 558–561.

(29) Kresse, G.; Joubert, D. From Ultrasoft Pseudopotentials to the Projector Augmented-Wave Method. *Phys. Rev. B* **1999**, *59*, 1758–1775.

(30) Kresse, G.; Furthmüller, J. Efficiency of ab-initio Total Energy Calculations for Metals and Semiconductors using a Plane-Wave Basis Set. *Comput. Mater. Sci.* **1996**, *6*, 15–50.

(31) Kresse, G.; Furthmüller, J. Efficient Iterative Schemes for ab initio Total-Energy Calculations using a Plane-Wave Basis Set. *Phys. Rev. B* **1996**, *54*, 11169–11186.

(32) Perdew, J. P.; Burke, K.; Ernzerhof, M. Generalized Gradient Approximation Made Simple. *Phys. Rev. Lett.* **1996**, *77*, 3865–3868.

(33) Tkatchenko, A.; Scheffler, M. Accurate Molecular van der Waals Interactions from Ground-State Electron Density and Free-Atom Reference Data. *Phys. Rev. Lett.* **2009**, *102*, 073005.

(34) Lüder, J.; Eriksson, O.; Sanyal, B.; Brena, B. Revisiting the Adsorption of Copper-Phthalocyanine on Au(111) Including van der Waals Corrections. *J. Chem. Phys.* **2014**, *140*, 124711.

(35) Lüder, J.; Sanyal, B.; Eriksson, O.; Puglia, C.; Brena, B. Comparison of van der Waals Corrected and Sparse-Matter Density Functionals for the Metal-Free Phthalocyanine/Gold Interface. *Phys. Rev. B* **2014**, *89*, 045416.

(36) Komeda, T.; Isshiki, H.; Liu, J. Metal-Free Phthalocyanine ($H_2Pc$) Molecule Adsorbed on the Au(111) Surface: Formation of a Wide Domain along a Single Lattice Direction. *Sci. Technol. Adv. Mater.* **2010**, *11*, 054602.

(37) Wang, J.; Davenport, A. J.; Isaacs, H. S.; Ocko, B. M. Surface Charge-Induced Ordering of the Au(111) Surface. *Science* **1992**, *255*, 1416–1418.

(38) Iski, E. V.; Jewell, A. D.; Tierney, H. L.; Kyriakou, G.; Sykes, E. C. H. Organic Thin Film Induced Substrate Restructuring: An STM study of the Interaction of naphtho[2,3-a]pyrene Au(111) Herringbone Reconstruction. *J. Vac. Sci. Technol., A* **2011**, *29*, 040601.

(39) Ibach, H. The Role of Surface Stress in Reconstruction, Epitaxial Growth and Stabilization of Mesoscopic Structures. *Surf. Sci. Rep.* **1997**, *29*, 195 – 263.

(40) Prévot, G.; Croset, B.; Coati, A.; Garreau, Y.; Girard, Y. Self-Organized Systems for Measuring Surface Stress at the Nanoscale: N and O Adsorption on Cu(001). *Phys. Rev. B* **2006**, *73*, 205418.

(41) Bach, C. E.; Giesen, M.; Ibach, H.; Einstein, T. L. Stress Relief in Reconstruction. *Phys. Rev. Lett.* **1997**, *78*, 4225–4228.

(42) Croset, B.; Girard, Y.; Prévot, G.; Sotto, M.; Garreau, Y.; Pinchaux, R.; Sauvage-Simkin, M. Measuring Surface Stress Discontinuities in Self-organized Systems with X Rays. *Phys. Rev. Lett.* **2002**, *88*, 056103.

(43) Shariati, M.-N.; Luder, J.; Bidermane, I.; Ahmadi, S.; Goethelid, E.; Palmgren, P.; Sanyal, B.; Eriksson, O.; Piancastelli, M. N.; Brena, B. et al. Photoelectron and Absorption Spectroscopy Studies of Metal-Free, Phthalocyanine on Au(111): Experiment and Theory. *J. Phys. Chem. C* **2013**, *117*, 7018.

(44) Nilson, K.; Åhlund, J.; Shariati, M.-N.; Göthelid, E.; Palmgren, P.; Schiessling, J.; Berner, S.; Mårtensson, N.; Puglia, C. Rubidium Doped Metal-free Phthalocyanine Monolayer Structures on Au(111). *J. Phys. Chem. C* **2010**, *114*, 12166.

(45) Sthr, M.; Wagner, T.; Gabriel, M.; Weyers, B.; Mller, R. Binary Molecular Layers of C60 and Copper Phthalocyanine on Au(111): Self-organized Nanostructuring. *Adv. Funct. Mater.* **2001**, *11*, 175–178.

(46) Liu, L. W.; Yang, K.; Xiao, W. D.; Jiang, Y. H.; Song, B. Q.; Du, S. X.; Gao, H.-J. Selective Adsorption of Metal-Phthalocyanine on Au(111) Surface with Hydrogen Atoms. *Appl. Phys. Lett.* **2013**, *103*, 023110.

(47) Kröger, I.; Stadtmüller, B.; Kumpf, C. Submonolayer and Multilayer Growth of Titaniumoxide-Phthalocyanine on Ag(111). *New J. Phys.* **2016**, *18*, 111002.

(48) Bidermane, I.; Luder, J.; Boudet, S.; Zhang, T.; Ahmadi, S.; Grazioli, C.; Bouvet, M.; Rusz, J.; Sanyal, B.; Eriksson, O. et al. Experimental and Theoretical Study of Electronic Structure of Lutetium Biphthalocyanine. *J. Chem. Phys.* **2013**, *138*, 234701.

TOC Graphic